HIGH PRECISION MINI-CMG'S AND THEIR SPACECRAFT APPLICATIONS

Jacques Busseuil,* Michel Llibre† and Xavier Roser*

Agility is a challenge for many future missions, especially for Low Earth observation. The growing need for commercial Earth images, especially with High Resolution, and the resulting narrow field of view, implies the development of satellites capable of rapid reorientation of their line of sight, such that the number of acquired images is increased and the accessibility is improved. The efficiency and cost-effectiveness of such system depend on these performances.

Agility of the line of sight can be achieved by either the maneuver capability of a part or of the complete instrument, or by the maneuver capability of the complete platform. This latter solution is less constraining for the often expensive and critical instrument but requires high torque and momentum capability.

Compared with the reaction wheels, the Control Moment Gyros (CMG's) are far more promising for such applications. The present paper analyses the requirements of such missions and details the adaptation of the Mini-CMG design to maneuvering applications : the wheel spin axis is supported by magnetic bearings to improve the reliability and precision of the actuator, the control is based on feedforward calculated steering laws, in order to use the maximal momentum envelope for the control.

Introduction

The purpose of this article is the evaluation of the application of Mini-Control Moment Gyros (CMG) to very stringent agile scientific missions, starting with the analysis of system driving requirements. For this purpose a reference optical Earth Observation mission is considered. On this basis promising improvements brought by the Mini-CMG technology wrt RW's are evaluated.

A new approach of singularity avoidance, based on a predictive CMG's kinematic calculation is proposed to allow a higher bandwidth CMG and satellite control, and an optimal use of the momentum capacity.

The application of AEROSPATIALE Magnetic bearing technology to the Mini-CMG's has been evaluated to improve the actuator accuracy by taking benefit of the bearing controlled flexibility.

* Mr. J. Busseuil, AOCS Department Manger, and X. Roser, Engineer responsible for AOCS advanced study, responsible for system, control and actuator design with Mini-CMG's, AEROSPATIALE, 100 Bd. du Midi, B.P. 99, F-06156 Cannes-la-Bocca Cedex, France. E-mail: xavier.roser@cannes.aerospatiale.fr.

† Mr. M. Llibre, Research Scientist, CERT ONERA, responsible for the steering law algorithm design, Complexe Scientifique de Rangueil, 2 Av. Edouard Belin, F-31400 Toulouse Cedex, France. E-mail: llibre@cert.fr.

System Overview

Typical Earth Observation Mission. Major Requirements

The main requirement for Earth observation is driven by the often used "Push-Broom" image acquisition technology. The detection is based on the use of one or several (to increase the radiometry) CCD lines, scanning the target image. Such instruments have severe high stability requirements necessary to ensure the image quality. The image quality is defined by the respect of the geometrical forms and distances implying low and mid frequency stability requirements ([0 – 40 Hz]) and the degradation of the contrasts, FTM (frequency higher than the sampling frequency). The FTM indicates the percentage of the received signal corresponding to the integrated pixels. The maximal value is 60%. The contribution of the instrument design to the FTM can be very high. These effects are explained by the following scheme (Fig. 1) :

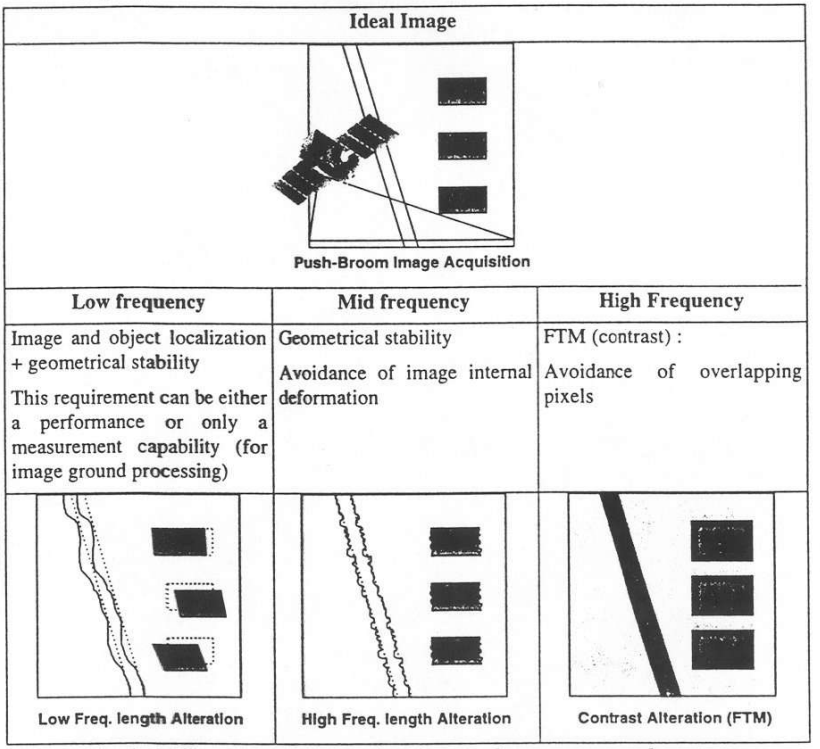

Fig. 1 : Different contribution to the image quality : geometry and contrast

Typical performances for a 2.5 m optical resolution instrument, composed of a single CCD line, are the following. They are very stringent (Fig. 2) :

FOV : ~ 30 km		
Localization : 250 m		
Stability Requirement		
5m/100m	10m/5000m	50% FTM
[0 , 0.5] Hz $7 . 10^{-4}$°/s	[0.5 , 20] Hz $2.5 . 10^{-4}$°	[20 , 250] Hz $3.5 . 10^{-2}$/s

Fig. 2 : Typical pointing requirements for a 2.5 m resolution Earth Observation Satellite

The scanning of a 30x30km image requires 5s. The repointing of the line of sight necessary for the Earth coverage and the access to the observation sites requires a rotation capability as high as possible of the satellite in order to minimize the duration between two images. A desirable performance is a repointing of 30° in less than 20s.

Typical satellite inertia for such mission are in the order of 500 $kg.m^2$ to 2000 $kg.m^2$, implying a Control Torque between 1 and 4 Nm and a momentum between 10 Nms and 35 Nms.

AOCS Design

The AOCS design of such an efficient satellite is closely related to the system design. The following main trade-offs and features have to be considered :

Actuator selection and sizing : Mini-CMG's vs. RWs

The torque and momentum requirements are above the today reaction wheel technology, implying either an excess of weight or of power consumption (and resulting thermal emission) of such an actuator. RW's are actually limited by their torque accuracy and power requirement.

The CMG's technology appears more efficient to perform such missions. As shown by the following figure (Fig. 3) [10], the torque and momentum requirements as expressed hereabove are not today covered by existing hardware.

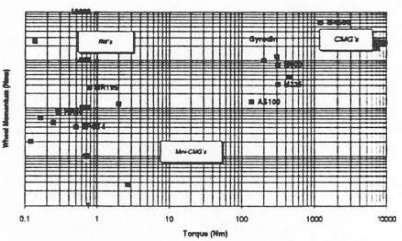

Figure 3 : Existing CMG's, RWs Momentum and Torque performances. A place for Mini CMG's

The CMG's main limitations (detailed below) are the following :

- Control Torque accuracy : this constraint is reduced thanks to the use of magnetic bearings, described below

- Configuration singularities reducing the momentum capability of a configuration, which implies the use of efficient steering laws and integrated control architecture as described in this article.

Sensors selection

The major limitation to the achievable satellite agility is the stability requirement. The increase of the torque/inertia ratio implies, the increase of the torque accuracy and stability of the actuator.

This constraint can be limited by increasing the control bandwidth (0.3-1 Hz). The sensitivity to the actuation uncertainties are thereafter reduced. This increase is made possible by the following element:

- High control torque capability (CMG's)
- Improved sensors : for instance HRG gyroscopes with a 10^{-4}°/s noise.
- Reduction of solar arrays flexible modes perturbation by increasing the frequencies and inertia of the structural modes, and the preferable use of fixed solar arrays. This system trade-off is made easier thanks to the agility making possible the rapid recovery of a Sun pointing attitude when no scan is commended.

Example of design : Advanced Earth Observation satellite

The use of CMG's has been considered for a vegetation observation satellite (Fig. 4) with stringent along track repointing requirements. The proposed design is one example of an agile satellite architecture

The design of an agile satellite requires to take closely into account the architecture.

- Reduction of the inertia, by a high integrated compact design
- Minimization of flexible modes impacts, by increasing their frequency and reducing their inertia. This is necessary to make high dynamics maneuvers accessible without having to support the flexible modes disturbances (pointing stability and high torque requirement), and to allow the relative high bandwidth of the control to reduce the effect of the CMG's torque uncertainties.

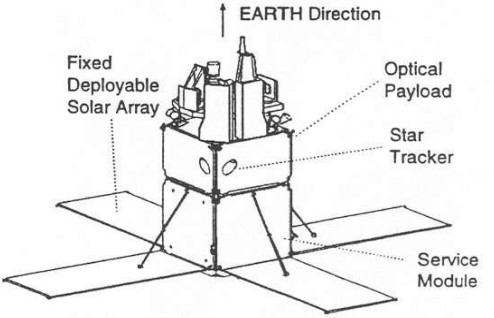

Fig. 4 :Example of agile Satellite Design for Earth observation

Actuator Technology

The feasability of the above described system performances requires the analysis of the sizing and design of a Mini-CMG.

H/W short description

A SGCMG (Fig. 5) is constituted of a momentum wheel, generating the angular momentum, **H**, mounted on a commandable gimbals axes.

The **input torque** of a CMG, which has to be generated to control the precession rate, $\dot{\alpha}$, is composed of the eigen torque needed to accelerate the precession rate and a gyroscopic cross-coupling torque, due to the rotation of the CMG's platform, $\dot{\theta}$:

$$T_{input} = \underbrace{I_G^{eff} \cdot \ddot{\alpha}}_{T_{eigen}} + \underbrace{H \cdot \dot{\theta}_X}_{T_{gyro}}$$

The **output torque** delivered to control the satellite is the following :

$$T_{output} = \underbrace{H \cdot \dot{\alpha}}_{T_{control}} + \underbrace{H \cdot \dot{\theta}_Y}_{T_{Gyro}}$$

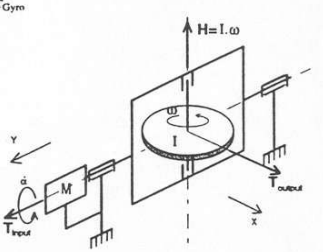

Fig. 5 : Principles of SGCMG

For a system of CMG's, the **resulting Gyroscopic torque on the spacecraft are null**, if the resulting momentum of the CMG's is null when the satellite has a null rotation rate.

CMG's Advanced model

Due to the flexibility of the whole gimbals structure, the input torque has to be sized for an efficient inertia, which depends of the momentum and of the overall stiffness :

$$I_G^{eff} = I_G + \frac{H^2}{k}$$

This efficient inertia has several impacts on the control law, which can be quite critical and this will be studied in the synthesis of the feedback control of the CMG's system.

As the stiffness of the gimbals structure is not infinite, the output torque generates a low frequency infinitesimal rotation of the momentum axis, which generates a resisting Torque on the input axis.

This flexibility effect is modeled by the following block diagram of a CMG [2]. The output Torque generates a deformation of the gimbals that generates an infinitesimal rotation of the momentum direction around the X axis. The cross coupling of this rotation with the momentum leads to a resistant torque on the Y-axis, the motor axis (Fig. 6).

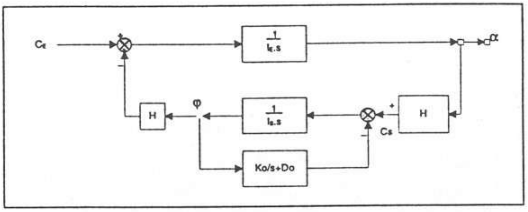

Fig. 6 : Flexible Block Model of a CMG

With the following notations,

$$\omega_1 = \sqrt{K_0/I_S}$$

$$\omega_2 = \sqrt{\frac{K_0}{I_S} + \frac{H^2}{I_E \cdot I_S}} = \sqrt{\frac{I_E^{eff}}{I_E}} \cdot \omega_1$$

$$\varsigma_1 = \frac{1}{2}\frac{D_0}{\sqrt{K_0/I_S}} = \frac{1}{2}\frac{D_0}{\omega_1}$$

$$\varsigma_2 = \frac{1}{2}\frac{D_0}{\omega_2}$$

$$I_E^{eff} = I_E + \frac{H^2}{K_0}$$

The CMG transfer function is consequently the following :

$$\frac{\dot{\alpha}}{C_E} = \frac{\frac{s^2}{\omega_1^2} + 2\varsigma_1 \cdot \frac{s}{\omega_1} + 1}{\frac{s^2}{\omega_2^2} + 2\varsigma_2 \cdot \frac{s}{\omega_2} + 1} \cdot \frac{1}{I_E^{eff} \cdot s}$$

This could first appear a drawback of the CMG system, but it is in fact a main advantage as long as the structure stiffness can be adjusted and is accurately known.

The CMG's motor is namely sized by:

$$C_{max} = I_{eff} \cdot \ddot{\alpha}_{max} + H \cdot \dot{\theta}^{Sat}_{max}$$

For agile spacecraft, with high rates, $H.\dot{\theta}$ is much higher than $I_{mec}.\ddot{\alpha}$, which means that a high T_{max}/T_{min} ratio i needed to comply with required accuracy. As the resolution of electrical gimbals drive motors is limited and proportionale to their maximal output torque, a high precision control of the gimbals rate can be achieved by increasing the apparent inertia of the gimbals.

This adjustment is limited by the frequency of its generated flexible mode, which must be 5 to 10 times higher than the bandwidth of the gimbals control. The necessary accurate knowledge of the gimbals stiffness can only be known by using magnetic bearings.

Adjustment of gimbals inertia with magnetic bearings

The use of magnetic bearings makes this adjustment possible. The stiffness of the bearing can be adjusted to a value 5 to 10 times smaller than the structure stiffness, especially for a mini-

CMG's. This reduced stiffness can increase of a factor 5 to 10 the mechanical inertia of the gimbals mechanism. This apparent inertia is known with an accuracy of 10%, which makes possible its efficient use to improve the accuracy of the CMG's Output torque (Fig.7).

⇨ The use of magnetic bearings on the rotor axis improves by a factor 5 the resolution of a CMG.

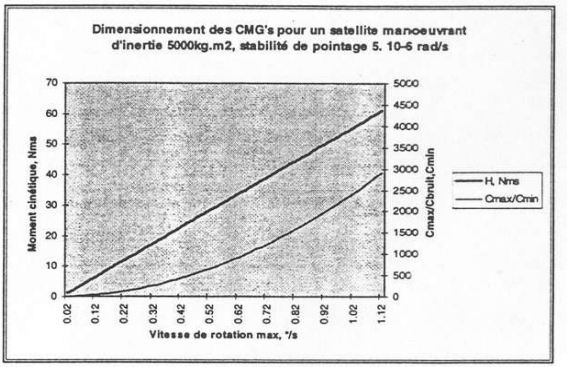

Fig. 7 : Sizing of a CMG

Mini-CMG design and foreseen characteristics

The system driving requirement has led to a design of a Mini-CMG. Most of the proposed technologies for the momentum wheel are derived from off-the shelf and already flown technologies, using the SPOT heritage.

The CMG's are based on a wheel rotating at a constant rate of 12 000 Rpm, and mounted on magnetic bearings. This wheel is mounted on a single axis gimbals mechanism. This mechanism is constituted by a supporting structure, and the gimbals actuation is made by an electrical motor. The rotating part is supported by ball bearings.

The following figure (Fig. 8) summarizes the main characteristics of this Mini-CMG's.

	CMG	SPOT 4 RW
Momentum	**50 Nms**	**40 Nms**
Output Torque	**30 Nm**	**0.45 Nm**
Wheel rate	12000 Rpm	2400 Rpm
Gimbals rate	0.6 rad/s	N/A rad/s
Gimbals acceleration	1.5 rad/s^2	N/A rad/s^2
Spacecraft maximum rate	2.5 °/s	N/A °/s
Gimbals Motor Output Torque	1.2 Nm	N/A Nm
Gimbals Torque Resolution	0.0024 Nm	N/A Nm
Weight with electronic	20 kg	17 kg
Wheel Inertia	0.0388 $kg.m^2$	_ $kg.m^2$
Gimbals mechanical inertia	0.0407 $kg.m^2$	N/A $kg.m^2$
Gimbals effective inertia	0.67 $kg.m^2$	N/A $kg.m^2$
Magnetic bearings stiffness	15 kNm/rad	0.46 kNm/rad
Run-up Power (16h)	90 W	N/A W
Stand-By Power	10 W	_ W
Quiescent Power	20 W	_ W
Peak Power	20 W	_ W

Fig. 8 : Compared characteristics of a reaction wheel and a Mini-CMG

This technical study demonstrates the feasibility of a Mini-CMG's. The main critical points are on the momentum wheel. Nevertheless the use of magnetic bearings to support the spin axis gives the system a high reliability, a high rotating speed that implies a weight reduction. An additional advantage of magnetic bearings is the reduction of μ-vibrations.

A prototype of this demonstrator, (Fig. 9) should be designed and tested in the near future.

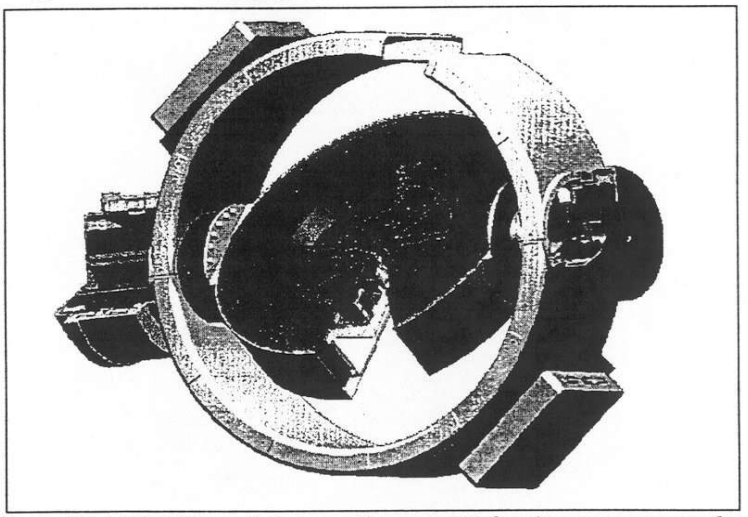

Fig. 9 : Mini-CMG Phase A design with a magnetic bearings momentum wheel

ADVANCED ACS Concept and Steering Law for high agile satellite

Notation

Some specific notations are necessary to describe the control with CMG's :

I_{Sat}	Spacecraft's inertia
Ω	Spacecraft's rotation rate
Ω_d	Spacecraft target rotation rate
P_i	Transfer Matrix between the CMG's frame and satellite frame
I_i^{CMG}	Inertia of the CMG number i
$\ddot{\theta}$	Satellite's acceleration
$\mathbf{T}_{ext}$	External torque's
$\mathbf{T}_{com}$	Control torque, output torque of the CMG's system
$\mathbf{T}_{gyro}$	Gyro-cross-coupling torque
$\mathbf{T}_{in}$	Inertial torque's
α_i	Precession position of the CMG number i
$\dot{\alpha}_i$	Precession rate of the CMG number i
$\mathbf{h}_i$,	Momentum of the i^{th} CMG
$\mathbf{H}_{tot}$	Total spacecraft angular momentum
$\mathbf{H}_S$	Spacecraft dynamic momentum
$M_{3xN_{CMG}}(\alpha_1, \ldots \alpha_{N_{CMG}})$	Configuration matrix
$\dot{h}_i$	Momentum variation (torque) of a reaction wheel
S	Singular Surface

Singularity and CMG's configuration

The main problem controlling a satellite with CMG's is the torque distribution to the actuator. The CMG are 2 axes actuator with only one degree of freedom. Consequently the design of a 3 axis control of a satellite with CMG's requires the use of at least 4 CMG's (recurring demonstration, 2 CMG's for one control axis, and a nominal 0 momentum). The amount of CMG's of the configuration has to be minimized for cost and weight purposes and wrt to the efficiency of the configuration (capability to use the maximal momentum envelope).

However such a configuration of CMG's can go through singularities [1]. A singularity is a set of gimbals (precession angles) for which the directions of output torque of all CMG's are in the same plane. It is at this point no longer possible to deliver a torque in the direction orthogonal to the plane (Fig. 10). Such a configuration is critical for the control and should be avoided.

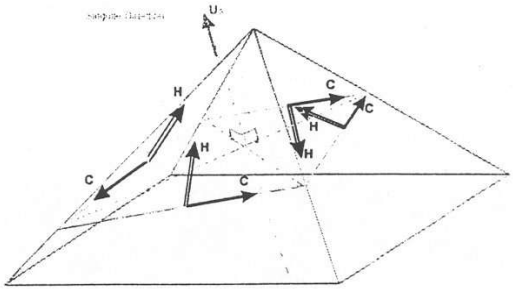

Fig. 10 : Classical Pyramidal configuration of a CMG's system. Singular configuration of a 4 CMG's system in a pyramidal configuration

Spacecraft dynamics with Control Moment Gyros

The CMG's are generally put on a pyramidal configuration (Fig. 10). The dynamic of a spacecraft actuated with CMG's (and eventually RWs) is the following :

$$\left(I_{Sat} + \sum_i P_i \cdot I_i^{CMG} \cdot P_i^T\right) \cdot \ddot{\theta} = T_{ext} + T_{com} + T_{gyro} + T_{in} \qquad . 1$$

The CMG's system output torque can be written :

$$T_{com} = -\sum_i \dot{\alpha}_i \wedge (P_i \cdot H_i) - \sum_j \dot{h}_j = M_{3xN_{CMG}}(\alpha_1, \ \dots \ \alpha_{N_{CMG}}) \cdot \begin{pmatrix} \dot{\alpha}_1 \\ \dots \\ \dot{\alpha}_{N_{CMG}} \end{pmatrix}$$

The output torque of the CMG system is a function of the geometry of the CMG's system and of the instantaneous position of the CMG's momentum. These parameters can be summarized by the **configuration matrix** : $M_{3xN_{CMG}}(\alpha_1, \ \dots \ \alpha_{N_{CMG}})$

Control and Singularity avoidance

The control of a satellite consists not only in the control of the satellite attitude, but also, and this is the most critical aspect, in the management of the CMG's precession angles.

All presented CMG's steering laws, gradient, indirect or direct avoidance, [2, 3] are local and global : they are based on the observation of the gimbals angles and the torque target at each sample time, and on generation of a global command of the gimbals rates. Their main principle consists in calculating the precession angles, considering the commanded torque, and the avoidance of singularities with the remaining degrees of freedom. All these solutions are composed of the superposition of a energy optimal term, calculated with the Moore-penrose Pseudo-inverse : $\dot{\alpha}_E = M^T(MM^T)^{-1}\dot{H}$ and of a null motion term, projected on the remaining degrees of freedom of the system of the singularity avoidance command. This remaining evolution of the gimbals angles does not provide any output torque.

These algorithms are all based on the determination of the nearest singularities direction, either by calculating all the singularities for the commanded torque direction (indirect avoidance) or by using a criteria (gradient) indicating the proximity of a singularity.

None of these algorithms has a sufficient robustness to make the complete momentum capability of a 4 CMG's configuration available, or a too high on-board calculation capability would be necessary. These algorithms are actually well adapted to stabilization applications, for which the evolution of the momentum is slow, and the encounter of a singularity results in a unvoidable momentum downloading command. These algorithms are also far more robust for a 6 CMG's configuration, with weight and cost consequences.

Maneuvering applications have rapid evolution of their momentum capability, limiting the calcultation capability and forbidding momentum down-loading. However they bring an additional information, the predictable evolution of the satellite momentum during the maneuver. On this basis a new steering law concept has been designed, consisting in the open-loop calculation of the precession angles target necessary to perform the commanded attitude change maneuvers. The resulting control architecture is described below before the control algorithms.

Control Architecture

The avoidance of singularity with a high control bandwidth and a high kinematics requires the implementation of a very efficient attitude control concept.

The proposed controller (Fig. 11) is thereafter based on the feedforward command of the precession angles added to a feedback control, using a classical Moore-Penrose Pseudo-inverse combined with a gradient type singularity avoidance laws to ensure a precise tracking of the commanded target profile.

The feedforward calculation of the precession angles is performed at a lower frequency and propagated, to limit the amount of calculation necessary to the maneuver.

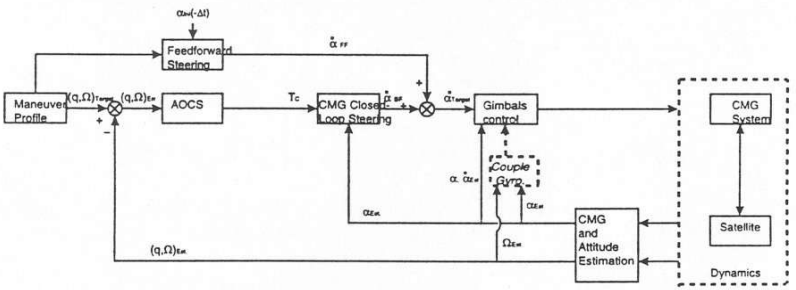

Fig. 11 : Control loop description of a satellite commanded with CMG's, with an openloop command of the precession angles.

Feedforward precession angles determination

As introduced above the steering of the CMG's configuration to perform maneuvers consists in finding an admissible gimbals angles trajectory, considering the "topology" of a CMG's system.

Momentum envelope and Singularities

The total angular momentum of the spacecraft can be divided into two parts :

$$H_{tot} = H_S(\Omega) + \sum_{i=1}^{n} h_i(\alpha_i)$$

- $H_S(\Omega)$ independent of the relative speed rate ω of the wheel
- $\sum_{i=1}^{n} h_i(\alpha_i)$, with $\|h_i\| = j\omega$, independent of the spacecraft angular velocity Ω.

Neglecting the exterior torque, we obtain :

$$h(\alpha) = \sum_{i=1}^{n} h_i(\alpha_i) = H_0 - H_S(\Omega) = H(\Omega)$$

where H_0 is a constant vector. From a *global steering* point of view the spacecraft's control consists in finding an admissible configuration trajectory $\alpha(t)$ so that

$$h(\alpha(t)) = H(\Omega_d(t)) \qquad (1)$$

where $\Omega_d(t)$ is the spacecraft's desired angular velocity trajectory. The total angular momentum $h(\alpha)$ is a mapping of the n-dimensional configuration space of the gimbal angles α_i into the physical space E_3.

For a given time t, this equation defines a n-3 dimensional manifold $\alpha_N(t)$ in the configuration space. It is called a null-motion (NM) manifold (NMM), or null-motion trajectory (NMT) in the $n = 4$ case. For increasing time t, equation (1) defines a n-2 dimensional manifold $\boldsymbol{H}$ on which (in the $n = 4$ case) the NMT form level lines corresponding to different times t. The admissible configuration trajectory $\alpha(t)$ belongs to this manifold $\boldsymbol{H}$ and crosses each NMM only once, with increasing time t.

By differentiating equation (1), one obtains :

$$\sum_{i=1}^{n} \frac{\partial h_i}{\partial \alpha_i} \cdot \dot{\alpha}_i = \mathbf{M} \cdot \dot{\alpha} = \dot{H}(\Omega) \qquad (2)$$

where vectors $\frac{\partial h_i}{\partial \alpha_i}$ and h_i have the same norm, are normal to each other and form a plane orthogonal to the gimbal axis. On a regular point the rank of jacobian $\mathbf{M}$ is 3. From a *local steering* point of view the spacecraft control consists in finding a good solution $\dot{\alpha}$ to this equation. This solution is the sum of two terms :

$$\dot{\alpha} = \dot{\alpha}_E + \dot{\alpha}_N$$

- $\dot{\alpha}_E$ is the Moore-Penrose pseudo-inverse solution of equation (2) :

$$\dot{\alpha}_E = \mathbf{M}^T \left(\mathbf{M}\mathbf{M}^T\right)^{-1} \dot{H}$$

- $\dot{\alpha}_N$ is any n-dimensional velocity configuration vector belonging to the null space of $\mathbf{M}$ wich is the tangent space of the null-motion manifold.

$\dot{\alpha}_E$ and $\dot{\alpha}_N$ are orthogonal. The trajectory $\alpha_E(t)$ obtained by the integration of $\dot{\alpha}_E$ is called an effective-motion (EM) trajectory (EMT). In the $n = 4$ case, EM and NM trajectories form a

rectangular meshgrid on $\boldsymbol{H}$. On this manifold, the EM trajectories are the shortest path to join two different NMM.

In the $n = 4$ case, NM trajectories form closed trajectories in the hyper-Torus T^4. For a given t, a NMT can be constituted by several separate sub-orbits. For example in the case of the semi-octahedron pyramid we can found NMT formed by 3 separate sub-orbits. From any initial point, the integration of $\dot{\alpha}_N$ gives an unique sub-orbit. To find all the orbits we can solve directly equation (1). To do it we choose one of the gimbal angles, say α_j, and solve the equation for the 3 others. This leads to a 8^{th} degree polynomial equation, and finally up to 8 different solutions $(\alpha_1, \alpha_2, \alpha_3, \alpha_4)$ for the same α_j. Inspecting a 2π range for α_j gives the whole NMT. Doing this for the whole domain of time t gives the whole surface $\boldsymbol{H}$.

On $\boldsymbol{H}$, we can find singular points. On a singular point the rank of M is less than 3. So it exists a direction u such that $u^T\mathbf{M} = 0$. In that configuration, the CMG cannot produce any torque along that direction. The null-space dimension being greater than 1 at that point, it corresponds to a crossing point of NM trajectories or their appearance or disappearance on $\boldsymbol{H}$. In the 4-dimensional configuration space, the singular points belongs to 8 singular surfaces $\boldsymbol{S}$ [1]. On $\boldsymbol{H}$, the singular points are at the intersections of surface $\boldsymbol{H}$ with these singular surfaces.

If $H(t)$ goes out of the boundary surface generated by vector $\sum_{i=1}^{n} h_i(\alpha_i)$, external singularity points on $\boldsymbol{H}$ are associated to the boundary surface. At the neighborhood of a such a point the NMT form closed trajectory rounding the singular point, and vanishing on it when t reaches the crossing time. This singular point is a elliptic point characterized by 2 positives eigenvalues (2+ signature) of the reduction of the quadratic form $u^T\delta h$ to the 2-dimensional null-space. In that case this signature corresponds to a 4+ signature of the whole quadratic form (w.q.f). For decreasing time, the singular point becomes a source where a new sub-orbits sequence arises. The singular point is always an elliptic point characterized by a 4- signature of the w.q.f. These singular points don't concern the spacecraft control, but has to be taken into account in the power design.

A sub-orbits sequence can vanish on an internal singular point. It is an elliptic singular point that can be obtained by a (3+, 1-) signature of the w.q.f. and negative gaussian curvature[1, 2] of the singular surface $\boldsymbol{S}$, or by a (2+, 2-) signature of the w.q.f. and positive gaussian curvature. For decreasing time, the vanishing point becomes a source where a new sub-orbits sequence arises. These elliptic singular point can be obtained by a (3-, 1+) signature of the w.q.f. and positive gaussian curvature of the singular surface $\boldsymbol{S}$, or by a (2+, 2-) signature of the w.q.f. and positive gaussian curvature.

Like external singular points, internal elliptic singular points found with increasing time are locally impassable. The solution trajectories go away from sources, and lead naturally to singular vanishing points. In the neighborhood of such, EM trajectories go straight ahead, by the shortest way, to the singular point.

At an hyperbolic singular point , two sub-orbits can join to form a bigger unique sub-orbit, or a sub-orbit can split to form two smaller sub-orbits. This hyperbolic singular point is characterized by a (1+, 1-) signature of the reduction of the quadratic form $u^T\delta h$ to the 2-dimensional null-space. This signature can be obtained by a positive gaussian curvature and a (3+, 1-) or (1+, 3-) signature of the w.q.f, or by a negative gaussian curvature and a (2+, 2-) signature of the w.q.f. In the neighborhood of such a point there is only one EMT who leads to

the singular point which is not attractive. Any EMT in the vicinity of this one does not go through the singular point. Any steering strategy takes away from that point.

Only internal elliptic (vanishing) points are a problem.

If, from a given initial state, this singular point is the only one rounded by the future sequence of sub-orbits, there is no way to escape. All trajectories will lead to that singular point. It is the same, if all singular points rounded by the future sequence are internal elliptic points. All trajectories will lead to one of these singular points. This situation will be called a dead end.

On the contrary, if there is also, at most one hyperbolic point, there is a way to escape as far as we don't go into a dead end. Local steering strategies have to avoid dead ends.

Singularity density

In the semi-octahedron pyramid case with $\|h_i\| = 1$, we have inspected the configuration space to characterize the density of internal singular points in vicinity of which pass by the effective motion trajectories. We present here the results for the starting configuration where all the four angular momentum axis are parallel to the base of the pyramid. From this (0,0,0,0) configuration where $H = 0$, we intend to produce a torque with a constant direction u, until we arrive at a point where $u^T(\mathbf{M}\mathbf{M}^T)^{-1}u > 25$. In comparison, when direction of u describes the whole unit sphere, we have $1.33 \le u^T(\mathbf{M}\mathbf{M}^T)^{-1}u \le 2.66$ at the starting point. For a little less than 30% of the directions of u, the EM trajectories lead to the vicinity of an internal singular point where the minimum value of $\|H\|$ is close to 1.13, and for a little more than 70% they lead to the boundary momentum envelope where $2.48 < \|H\| < 3.26$. This result is shown on fig. 12.

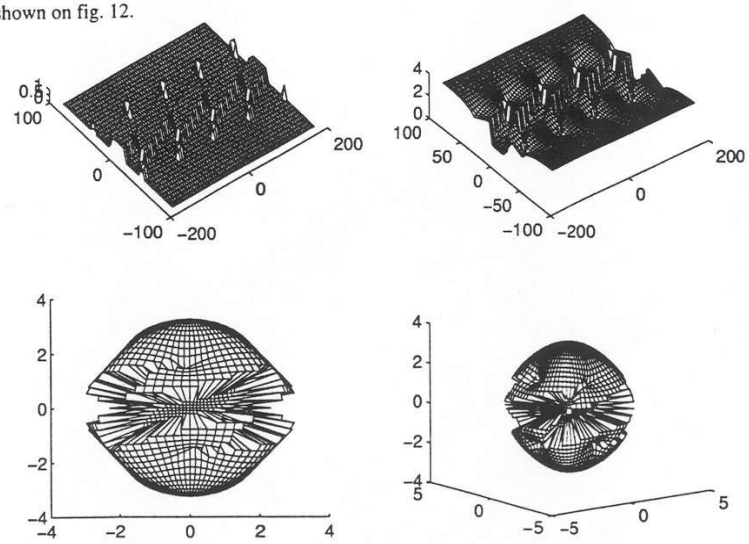

Fig. 12 : Singularities reached by effective motion trajectories from (0,0,0,0)

The two bottom frames show the surface formed by the reached angular momentum. It looks like a sphere with a 3.26 maximum radius and a 1.13 minimum radius in the equatorial valley. The left frame is a front view of the X_OZ_O plane.

The top-right frame represents the altitude of the same surface on a map with orthogonal meridians and parallels.

On the top-left frame, the altitude of the map is 1 when the reached singular point is internal or 0 when it is on the boundary envelope (external).

A surface *H* analysis

Figure 13 shows surface ***H*** corresponding to a $\vec{H}_d(\Omega) = t\vec{X}_O$ desired trajectory, where $\vec{X}_O$ is a unit vector parallel to the base of the pyramid and orthogonal to a side.

For $t = 0$, the NMT parametric equations are $(a,-a,a,a)$, $(a,\pi+a,a,\pi+a)$, $(a,\frac{\pi}{3}+a,-\frac{\pi}{3}-a,-a)$ and $(a,-a,\frac{\pi}{3}-a,a-\frac{\pi}{3})$, where a is the parameter. In the hyper-torus T^4, they form different sub-orbits that cross at the following hyperbolic singular points : $(\frac{\pi}{2},-\frac{\pi}{2},\frac{\pi}{2},-\frac{\pi}{2})$, $(-\frac{\pi}{2},\frac{\pi}{2},-\frac{\pi}{2},\frac{\pi}{2})$, $(-\frac{\pi}{6},\frac{\pi}{6},-\frac{\pi}{6},\frac{\pi}{6})$, $(\frac{5\pi}{6},-\frac{5\pi}{6},\frac{5\pi}{6},-\frac{5\pi}{6})$, $(\frac{\pi}{6},-\frac{\pi}{6},\frac{\pi}{6},-\frac{\pi}{6})$, $(-\frac{5\pi}{6},\frac{5\pi}{6},-\frac{5\pi}{6},\frac{5\pi}{6})$. As soon as t increases, each NMT has 2 different sub-orbits that form 2 tubes in the hyper-torus (some tubes are drawn several times because of the 2π modulo) .

For $t \approx 0.82$ (with $\|h_i\| = 1$) the biggest tube splits into two smaller ones at the hyperbolic singular points $E = (\frac{\pi}{2},\pi,-\frac{\pi}{2},0)$.

For $t \approx 1.14$ these two tubes merge with the other one, and split into 3 new tubes at 4 hyperbolic singular points C near $B_1 = (-\frac{\pi}{2},0,\frac{\pi}{2},0)$ and $B_2 = (-\frac{\pi}{2},\pi,\frac{\pi}{2},\pi)$

For $t \approx 1.1547$ two of the new tubes vanish at the internal elliptic singular points B_1 and B_2.

For $1.1547 < t < 3.1547$, it remains only one tube that leads to the external elliptic singular point $D = (-\frac{\pi}{2},\pi,\frac{\pi}{2},0)$.

Starting from $A = (0,0,0,0)$ the effective motion trajectory leads straight ahead to the internal elliptic singular point B_1. To avoid this attractive singularity the trajectory should pass near the hyperbolic singular points C to leave the initial tube and go to the one that leads to D.

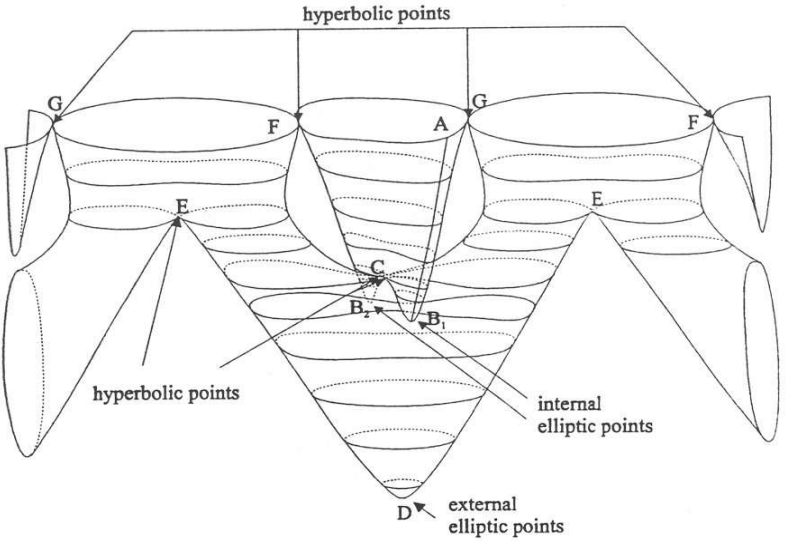

Fig. 13 :. H *surface for* $\vec{H}_d(\Omega) = t\vec{X}_o$

The topology analysis of such surfaces leads us to consider the following steering strategies.

First, for a given desired spacecraft attitude trajectory, we have to calculate an optimal trajectory $\hat{\alpha}(t)$ going from the initial point to the NMT corresponding to the final time, calculated by forward dynamic programming. Then, in a first approach, the null-space of **M** will be used to add to the term $\dot{\alpha}_E$ (calculated to produce the desired control torque) a term that drawn towards the nominal configuration $\hat{\alpha}(t)$. Another approach is to use the derivative $\frac{d}{dt}\hat{\alpha}(t)$ as a feed-forward term to produce the reference control torque profile. This global strategy supposes that we know in advance the desired attitude trajectory and have time to implement the dynamic programming algorithms.

Conclusion

The CMG's technology remained confidential during a long time and limited to large spacecraft stabilization and maneuvers, due to limitation of the torque accuracy and of the difficulty to implement on-board the singularity avoidance laws.

The use of a magnetic bearings momentum wheel should make possible the design of a far more accurate actuator, and will support higher rotation rates of the satellite.

Moreover new singularity steering laws, calculated in open-loop according to the maneuver profiles make possible to perform rapid repointing of the platform and to use the complete momentum potential of the CMG's configuration, improving the satellite design.

Mini-CMG's can also be used for stabilization of large satellite. like ENVISAT or Large Space Telescopes (FIRST, XMM ...). These applications less stringent were not considered in the present paper.

The technical results based on AEROSPATIALE experience in the SPOT magnetic bearing wheels should be consolidated by the testing of a prototype mini-CMG in the near future.

Acknowledgment

We would like to thanks especially the :

- **CERT** team who worked on the CMG steering laws design.
- French and European agencies, **CNES, DME, ESA** who are contributing by their foundings and own studies to the Mini-CMG's development.
- **AEROSPATIALE** magnetic bearings, mechanisms and electronic engineers (J.P. Roland, P. Vezain, C. Walstein) for their contribution in the hardware design.

For their contribution in the CMG's studies.

Reference

1. G. Margulies and J.N. Aubrun.:"Geometric Theory of Single-Gimbal Control Moments Gyro Systems " . Journal of the Astronauticals Sciences, Vol XXVI, No. 2, pp. 159-191, 1978.
2. H. Kurokawa. : "Exact Singularity Avoidance Control of the Pyramid Type CMG System". AIAA-94-3559-CP, pp. 170-180, 1994.
3. Singularity Avoidance Control Laws for SGCMG, D.E. Cornik, AIAA Paper 79-1698, 1979
4. Precision CMG Control For High Accuracy Pointing, Linden S.P. J. of Spacecraft Vol.11, No.4, 1974
5. Flight Performance of Skylab Attitude and Pointing System, Chubb, W.B.; Kennel, H.F.; AIAA Guidance and Control Flight Conf., 1974.
6. Ultrahigh-Accuracy Body Pointing for the Large Space Telescope, Rybak, S.C., Mayo, R.A.; J. of Spacecraft, Vol.13, No.4, 1975
7. Magnetically-Suspended Momentum Gyro for Orbital Space Stations Attitude Control, Veinberg D.M., N.N Shermetyevsky, V.P. Vereshchagin, IAF-1981
8. Slewing Maneuvres and Vibration Damping of Space by feedforward/ Feedback Moment-Gyro Controls, Yang L., J. of Dynamic System, 1995
9. Space Infrared Telescope Facility/Multimission Modular Spacecraft Attitude Control System Conceptual design., Welch R.V., AAS86-031
10. Small-CMG's. Needs, Capabilities, Trades and Implementation. Blondin, J.C.; AAS96-052